JOURNAL OF MATERIALS SCIENCE 27 (1992) 4842–4846

Nucleation sites of the T_2 phase in alloy 2090

E. A. LUDWICZAK, R. J. RIOJA
Alcoa Laboratories, Alcoa Center, PA 15069, USA

Alloy 2090 fabricated as O-Temper sheet exhibited the presence of the T_2 phase. The morphology and nucleation characteristics of the T_2 phase in alloy 2090 were investigated by transmission electron microscopy. Also, the crystal structure was documented by electron and X-ray diffraction analyses. It was found that T_2 precipitates formed preferentially at the interface of heterogeneities in the alloy. Several types of heterogeneities were identified. From these results it was proposed that as the impurities are eliminated, the propensity for nucleation of the T_2 phase should be reduced.

1. Introduction

Foils prepared from 2090-0 temper sheet were examined by transmission electron microscopy (TEM). In these foils the dominant precipitate found was the T_2 phase. It has been reported that, in alloy 8090, the presence of the T_2 phase is deleterious to the mechanical properties [1]. However, in alloy 2090-0 temper sheet the T_2 phase is associated with excellent formability. This study was undertaken to document the nucleation characteristics of the T_2 precipitates. The T_2 phase was first reported by Hardy and Silcock [2]. In their investigation a crystal structure for this phase was not determined. It was noted, however, that X-ray diffraction patterns revealed that the T_2 phase was not cubic. Recently many investigators have reported that the T_2 phase exhibits five-fold (icosohedral) symmetry. Since these findings contradict long-standing beliefs, two schools of thought have developed. One school maintains that the icosohedral structure is real, whereas others maintain that this is not a real structure, but rather that the five-fold symmetry results from double diffraction arising from very fine cubic or rhombohedral crystallites [3, 4].

2. Experimental procedure

Foils were first produced in a Struers Twin Jet electropolisher using a solution of 23% nitric acid in methanol cooled to $-30\,^{\circ}C$. Examination of these foils was done on a Philips EM420 microscope operating at 120 kV, having an energy-dispersive analysis by X-rays (EDAX) detector, with a beryllium window, and a Tracor Northern analyser. Also, a portion of this investigation was done on a Philips EM420 microscope, equipped with a Kevex unit, having a windowless detector. This allowed the detection of elements with atomic number as low as 4. Approximately 10–15% of the total number of the T_2 particles contained a central region which, in the bright-field mode, exhibited little or no diffraction contrast. Since this feature could be attributed to a polishing artefact, new foils were prepared on a Gatan dual-gun ion-mill having a liquid-nitrogen-cooled stage. These thin-foil specimens were then examined on the microscope and found to contain the same type of particle, thus eliminating the possibility that this feature was a result of a polishing artefact. As an adjunct to this investigation, a stoichiometric melt of the T_2 phase was cast and slowly cooled in an open-air furnace to grow the T_2 phase. This casting was then used to generate diffraction data by the X-ray Guinier–de Wolff technique [5].

3. Experimental results and discussion

Examination of the ion-milled foils revealed that the T_2 phase particles were identical to those first observed in the electropolished thin foils. The majority of the T_2 particles exhibited a solid globular morpho-

TABLE I X-ray Guinier–de Wolff analysis of the T_2 phase compared with Hardy and Silcock [2]

d (nm)	Intensity, visual	Computed d[a] (nm)	hkl	d from [2] (nm)	Intensity[b]
1.025	5	1.0359	1 1 0		
0.592	15	0.5980	2 1 1	0.591	W
0.425	10	0.4229	2 2 2	0.424	S
0.367	10	0.3662	4 0 0		
0.344	5	0.3453	3 3 0		
0.312	2	0.312	3 3 2		
0.238	50	0.2376	6 1 1	0.236	M
0.2265	100	0.2260	5 4 1	0.225	S
0.199	50	0.1993	7 2 1	0.197	MS
0.192	40	0.1923	7 3 0	0.192	MW
0.162	10	0.1617	9 1 0	0.164	W
0.1395	60	0.1396	10 3 1	0.139	S
0.1325	10	0.1326	11 1 0		
0.130	10	0.1305	11 2 1	0.129	W
0.1185	15	0.1180	12 3 1	0.1192	MW
0.1125	2	0.1123	13 1 0	0.1065	MS
				0.1053	W
				0.0927	W

[a] Computed d-spacings for bcc structure with $a = 1.465$ nm.
[b] W, weak; M, medium; and S, strong.

0022–2461

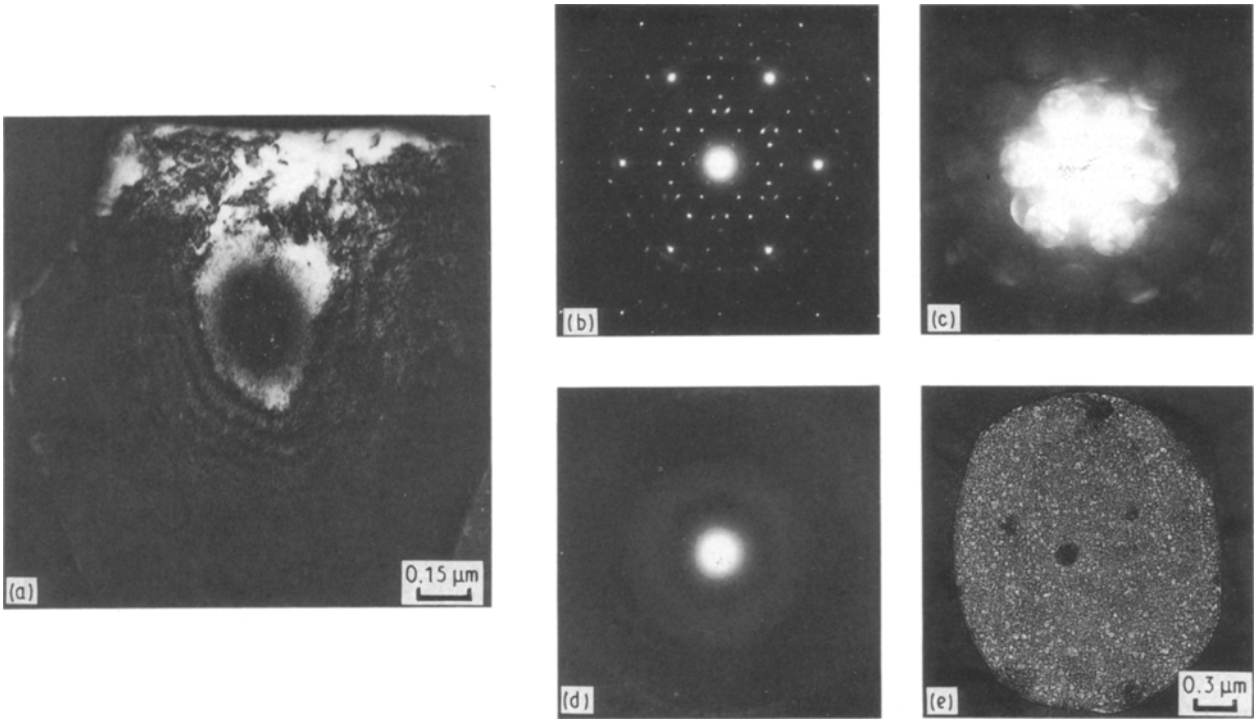

Figure 1 (a) Dark-field image of T_2 particle with core, (b) three-fold diffraction pattern from bulk of particle, (c) corresponding CBEDP, (d) SADP from core of particle and (e) dark-field image of core at higher magnification obtained from innermost ring of (d).

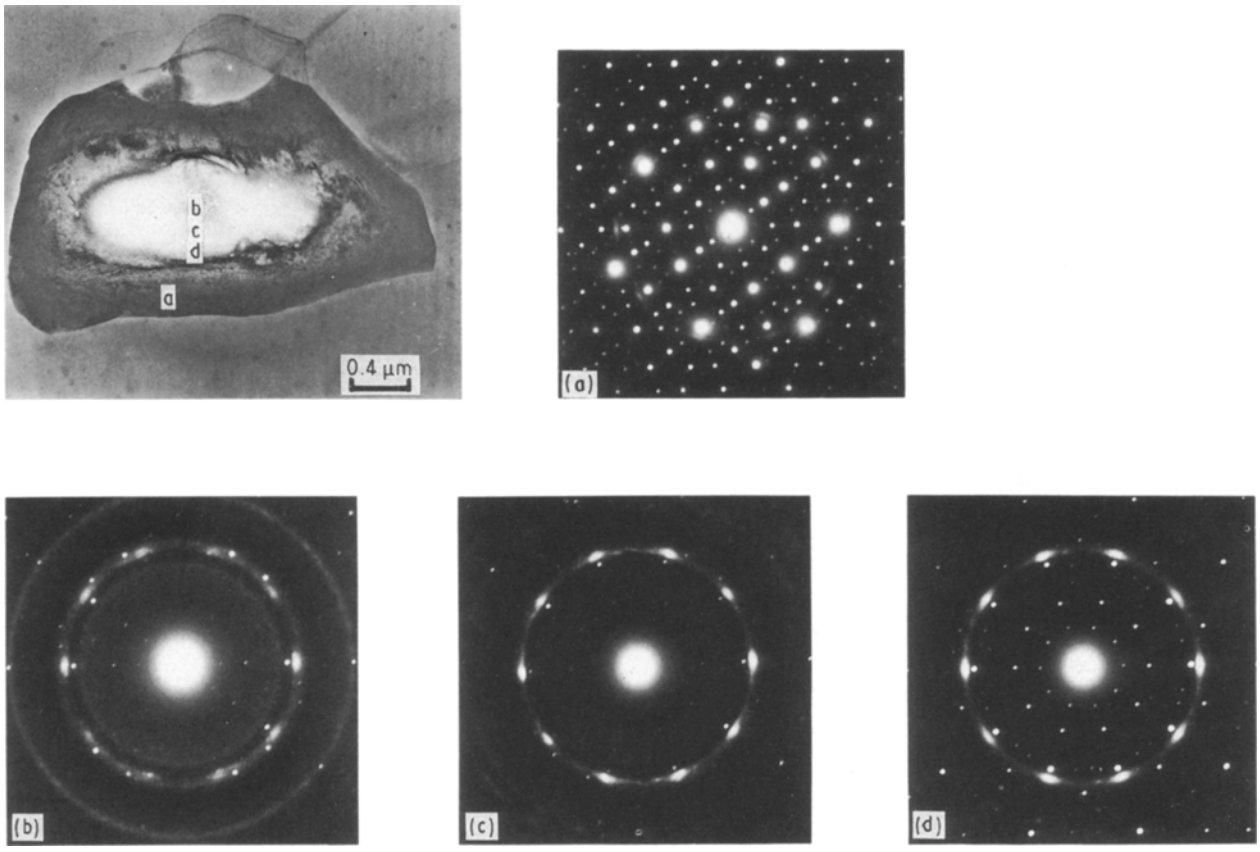

Figure 2 Bright-field micrograph of cored T_2 particle showing extensive area of core. (a) Five-fold diffraction pattern obtained from bulk of T_2 particle, (b) SADP from centre of core, (c) SADP from midway between centre and edge of core and (d) SADP from near edge of core.

logy. These particles ranged from 1.5 to 2.5 μm in size. In bright field the particles exhibited a striated appearance of alternating light and dark regions suggestive of strain contrast. In addition, there were particles with a different morphology. These particles differed in that the T_2 particle contained a central region that was featureless in the bright-field mode. Also, this region exhibited little or no diffraction contrast during tilting. This type of T_2 particle is here designated as the "cored" particle and the featureless region is called the

"core". It is these cored particles that were the subject of this investigation.

Table I shows the results of the X-ray diffraction analysis of the stoichiometric melt sample. The data show the measured d-spacings from the X-ray film. These measurements are contrasted with computed d-spacings based on the body-centred cubic (bcc) structure with $a = 1.465$ nm. Note also the results from Hardy and Silcock [2], which show a good correlation.

The majority of the core regions produced selected-area diffraction patterns (SADPs) that exhibited diffuse rings as shown in Fig. 1e. Fig. 1d is the dark-field image produced from the innermost ring of the pattern. Note that the dark-field image shows the presence of very fine crystallites. Fig. 1b and c shows the SADP and the convergent-beam electron diffraction pattern (CBEDP), respectively, obtained from the solid globular area of the T_2 particle. These show the characteristic three-fold pattern of the T_2 phase. Fig. 1a shows the dark-field obtained from a reflection of the three-fold pattern. Note that only some regions of the T_2 particle are imaged in dark-field from an individual reflection. Figs 2–4 show results from another T_2 particle. Fig. 2a shows a typical five-fold pattern obtained from the solid portion of the particle as indicated by the arrow. Fig. 2b, c and d show a series of SADPs obtained from different areas of the core region. Fig. 2b shows the pattern obtained from the centre of the core region. Note that here the pattern exhibits diffuse rings with some discrete spots, which is characteristic of a microcrystalline structure. Fig. 2c shows the pattern obtained from approximately midway between the centre and the edge of the core. The point of interest here is that the outer ring has faded and the discrete spots of the inner ring have separated into 10 distinct maxima. Fig. 2d shows the pattern obtained from the edge of the core. Here the pattern exhibits the 10-maxima ring together with some of the spots from the five-fold pattern of the solid

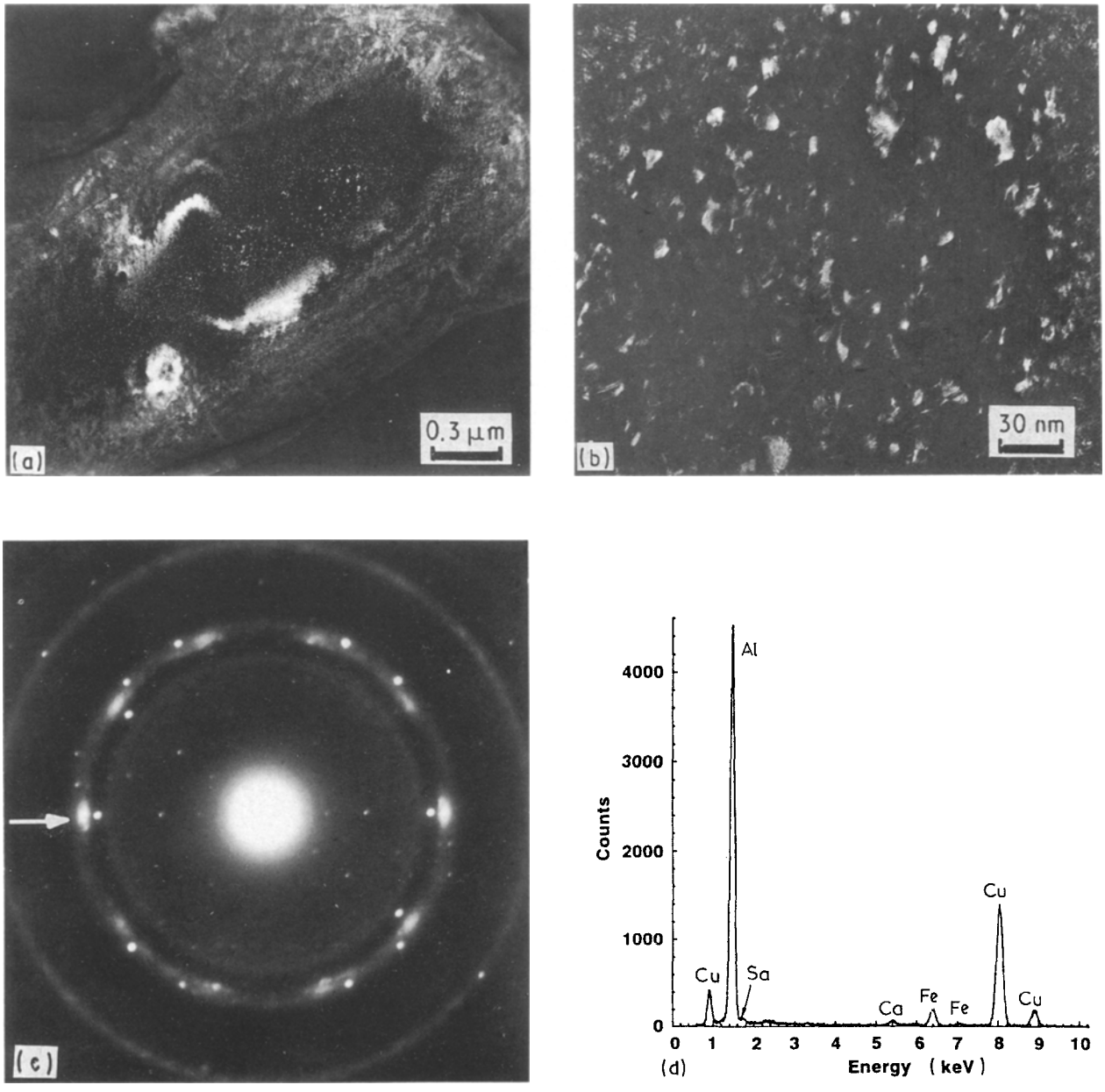

Figure 3 (a) Dark-field image of core obtained from maxima indicated in (c), (b) higher-magnification of core shown in (a), (c) SADP from core region and (d) EDAX spectrum from centre of core.

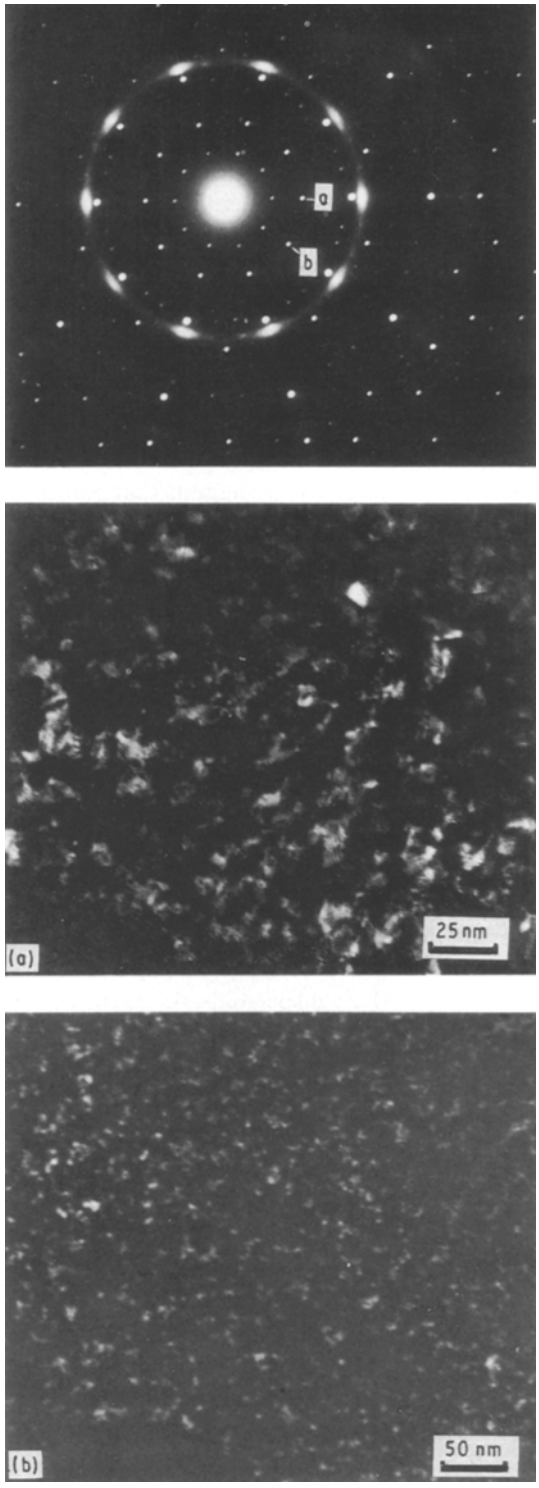

Figure 4 SADP from edge of core in Fig. 2 with dark-field micrographs obtained from the indicated reflections.

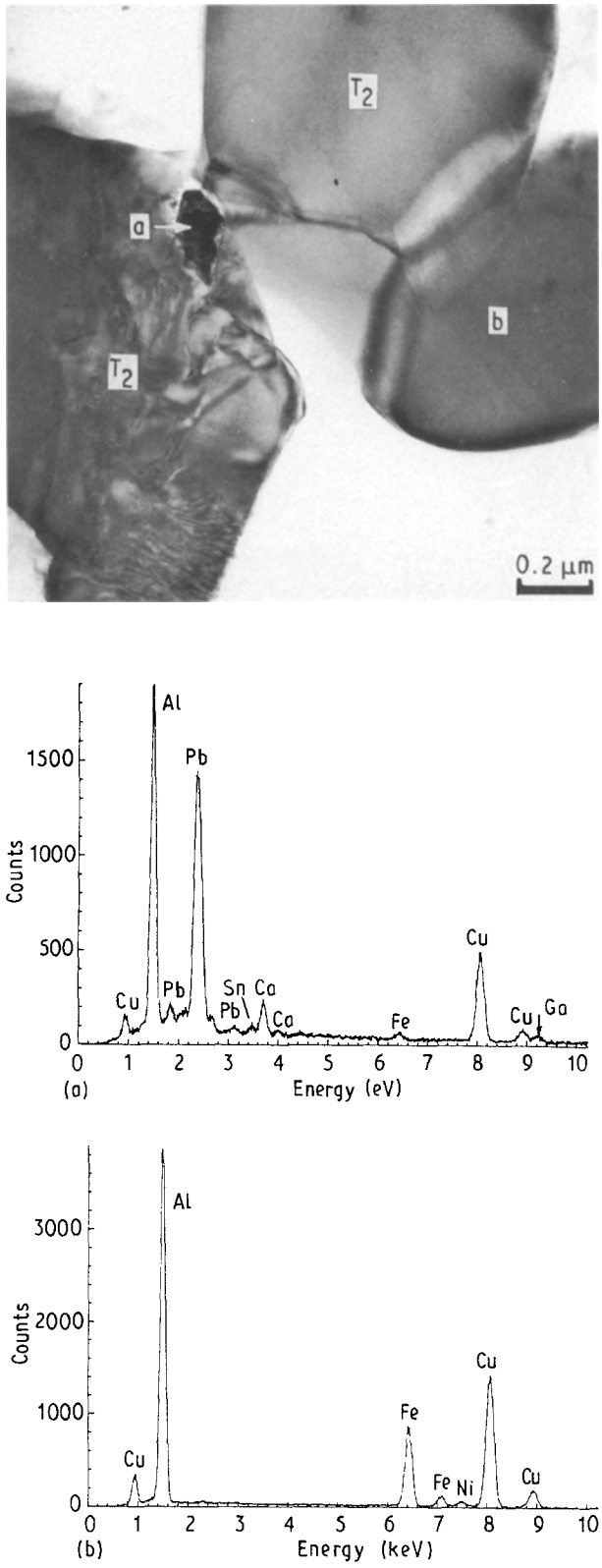

Figure 5 Bright-field micrograph of two T_2 particles identified by electron diffraction and spectra from two nucleating particles.

part of the T_2 particle. The obvious angular relationship of the maxima and the discrete spots suggest an epitaxial relationship between the core and the solid particle. Fig. 3a shows a dark-field image obtained from one of the 10 maxima of the inner ring. This shows that the core comprises fine crystallites. These crystallites averaged 5 nm in size. A spectrum obtained from the core region is also shown. Fig. 4 shows the dark-field micrographs obtained from two adjacent reflections of the five-fold pattern. The lower left quadrant of both of these micrographs is the core region. Note here that the different reflections image different crystallites in the solid portion of the particle. In a recent investigation of the icosohedral phase that forms in rapidly solidified Al–Mn alloys a diffuse ring diffraction pattern was reported [6]. Also, fine crystallites were observed in dark-field micrographs obtained from the rings. From this evidence it was concluded that the diffuse ring pattern was not indicative of an amorphous structure but was due to zones of the

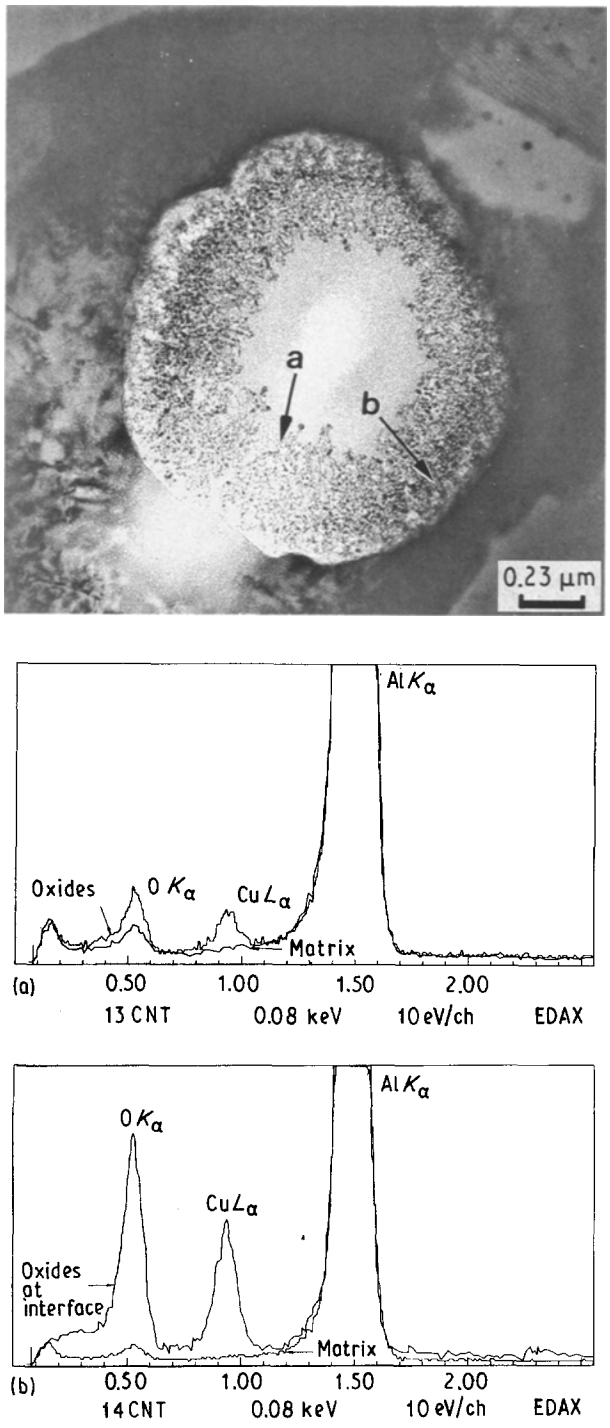

Figure 6 EDAX spectra from two regions of core that exhibited diffuse rings in SADP. Spectra are plotted against spectra obtained from nearby matrix.

order of 1–2 nm in size which exhibited a "micro-quasicrystalline" structure. However, in this investigation the micro-quasicrystalline structure cannot be supported since measurements of the diffuse ring patterns do not conform to a Fibonacci series.

Some T_2 particles were observed on the interfaces of other particles. Fig. 5 is an example of this. Note the two particles labelled T_2 (identified by electron diffraction) adjacent to two other particles. The spectra from each of the other two particles are indicated by arrows in Fig. 5. The spectrum from the larger of the two particles is characteristic of that normally obtained from Al_7Cu_2Fe constituents, whereas the spectrum from the smaller particle indicates the presence of several impurity elements. Since the Al_7Cu_2Fe forms before the T_2 phase, this suggests that these particles act as preferential nucleation sites for the T_2 phase.

To clarify further the nature of the core region of the T_2 particles, a Philips EM420 microscope equipped with a Kevex unit with a windowless detector was used. A T_2 cored particle that generated a diffuse ring pattern from the core was selected for this examination. Spectra obtained from two different areas of the core region are shown in Fig. 6. Here the spectra obtained from the core are plotted against a spectrum obtained from the matrix area immediately adjacent to the solid portion of the T_2 particle. The upper plots in both spectra are from the core regions indicated by the arrows. These indicate the presence of a greater amount of oxygen in the core region compared within the bulk of the sample. This suggests that oxides act as nucleating sites for T_2 precipitates. Since it is known that non-metallic inclusions were abundant in Al–Li alloys fabricated in the early 1980s, it is speculated that the nucleation of the T_2 phase on these inclusions could contribute to the poor fracture toughness of these alloys. In addition, it was found that in a few of the core regions a cluster of Al_3Zr dispersoids was present.

4. Conclusions

The above observations indicate that T_2 precipitates nucleate at a variety of sites as: particles of aluminium–lithium oxides, clusters of alkali and other impurities, Al_7Cu_2Fe constituent particle interfaces and clusters of Al_3Zr dispersoids. T_2 particles exhibit two distinct morphologies: solid and cored. The solid particles constitute the majority of the precipitates observed. The cored particles reflect nucleation sites of the T_2 phase. The angular coincidence of the ring pattern maxima of the core and the discrete spots from the bulk of the particle suggests an epitaxial relationship between the core and the bulk. It is proposed that as impurities were eliminated in this alloy, the propensity of the nucleation of T_2 precipitates was reduced and this resulted in improved fracture toughness.

Acknowledgements

The author acknowledges that the casting of the stoichiometric melt was accomplished by Dr Men Glen Chu and the X-ray results were generated by Mr J. C. Casato.

References

1. G. N. COLVIN and E. A. STARKE, Jr, *SAMPE Q.* **19**(4) (1988) 10.
2. H. K. HARDY and J. M. SILCOCK, *J. Inst. Met.* **84** (1955–56) 424.
3. L. PAULING, *Lett. Nature* **317** (10 October 1985) 512.
4. A. M. AUDIER and P. GUYOT, *Acta Metall.* **36** (1988) 1321.
5. L. A. BENDERSKY and S. D. RIDDER, *Mater. Res. Soc. Symp. Proc.* **80** (1987) 349.

Received 9 April
and accepted 1 August 1991